General Patterns of the Phase Behavior of Mixtures of H_2O, Nonpolar Solvents, Amphiphiles, and Electrolytes. 2

M. Kahlweit,* R. Strey, R. Schomäcker, and D. Haase

Max-Planck-Institut für Biophysikalische Chemie, Postfach 2841, D-3400 Göttingen, FRG

Received July 19, 1988. In Final Form: October 5, 1988

In part 1 of this series (ref 1) we presented a qualitative thermodynamic description of the phase behavior of quaternary mixtures of water, nonpolar solvents, nonionic amphiphiles, and salts. The phase behavior of such mixtures follows general patterns that are essentially determined by the phase diagrams of the corresponding binary and ternary mixtures. In this paper (part 2) the nonionic amphiphiles are replaced by ionic amphiphiles. The general patterns of these mixtures, in particular the phase sequence with rising temperature, are inverse to those with nonionic amphiphiles.[3] It is shown that this inverse behavior originates from the difference between the phase diagrams of binary H_2O–nonionic amphiphile and those of H_2O–ionic amphiphile mixtures.

I. Introduction

Mixtures of water, oils, amphiphiles, and salt may separate into three coexisting liquid phases within a well-defined temperature interval, the mean temperature of which depends sensitively but systematically on the nature of the oil and of the amphiphile and on the salt concentration. At the mean temperature of this interval one finds—for thermodynamic reasons—a maximum of the mutual solubility between water and oil and a minimum of the interfacial tension between the aqueous and the oil-rich phase. As both properties are of considerable interest for both research and industry, we ask where to find the three-phase bodies. The phase behavior of mixtures with nonionic amphiphiles can be considered as being clarified.[1,2] In this paper the nonionic amphiphiles (C) are replaced by ionic amphiphiles (D). Accordingly, we consider quaternary mixtures H_2O (A)–oil (B)–ionic amphiphile (D)–salt (E). Again we keep the pressure constant and introduce as composition variables the mass fraction of the oil in the mixture of water and brine

$$\alpha \equiv B/(A + B + E) \tag{1}$$

that of the ionic amphiphile in the mixture of all four components

$$\gamma \equiv D/(A + B + D + E) \tag{2}$$

and that of the salt in the brine

$$\epsilon \equiv E/(A + E) \tag{3}$$

all expressed in weight percent (wt %).

The phase behavior of A–B–D–E mixtures becomes more transparent if discussed in comparison with A–B–C–E mixtures as summarized in ref 1. Let us first consider ternary A–B–C and A–B–D mixtures, respectively, without salt ($\epsilon = 0$). The major difference between the phase behavior of mixtures with nonionic and with ionic amphiphiles lies in the inverse temperature dependence of the distribution of the amphiphiles between water and oil. Nonionic amphiphiles are more soluble in the lower aqueous phase ($\underline{2}$) at ambient temperatures but more soluble in the upper oil-rich phase ($\bar{2}$) at elevated temperatures. With ionic amphiphiles, the inverse is true. This is demonstrated in the top part of Figure 1, which shows the volume fraction $\phi_a = V_a/V$ of the (lower) aqueous phase (a) versus temperature T for the mixture H_2O–toluene–$(C_8)_2$DABr, the latter standing for dioctyldimethylammonium bromide. If compared with the corresponding curve for an A–B–C–mixture (left part of Figure 2 in ref 1), one finds that ionic amphiphiles are more soluble in the upper oil-rich phase ($\bar{2}$) at low temperatures but more soluble in the lower aqueous phase ($\underline{2}$) at high temperatures.

This result implies that the critical line that ascends along the surface of the body of heterogeneous phases changes from the water-rich to the oil-rich side with rising temperature, as schematically shown in the bottom of Figure 1, thus exhibiting an inverse temperature dependence as that of the critical line in an A–B–C mixture (Figure 1 in ref 1). This inverse temperature dependence can be readily understood if one considers the phase diagrams of the corresponding binary mixtures. Figure 2 shows the unfolded phase prism of an A–B–D mixture with schematic phase diagrams of the corresponding binary mixtures, to be compared with Figure 4 in ref 1. The phase diagrams of the A–B mixtures are, of course, identical. The phase diagrams of the B–C and B–D mixtures are rather similar. Both show a single (lower) miscibility gap only. The critical temperature T_α depends on the nature of both the oil and the amphiphile. For a given amphiphile, T_α rises with increasing (effective) carbon number of the oil, whereas for a given oil it rises with increasing hydrophilicity of the amphiphile. Accordingly, T_α may vary from temperatures below the melting point to such above the boiling point.

The major difference between nonionic and ionic amphiphiles exhibits itself in the phase diagrams of the A–C and the A–D mixtures, respectively. The critical point of the lower A–C gap lies (for single-tailed nonionic amphiphiles) below the melting point and plays no role in the further discussion. At ambient temperatures, water and nonionic amphiphiles are completely miscible (disregarding anisotropic mesophases at high amphiphile concentrations at this point). With rising temperature, however, water becomes an increasingly poorer solvent for nonionics. As a consequence, the A–C mixture separates again into two isotropic liquid phases at a lower critical point, the temperature T_β of which rises with increasing hydrophilicity of the amphiphile. At a temperature close to T_β, nonionic amphiphiles, therefore, become more soluble in oil than in water, which makes the critical line change from the oil-rich to the water-rich side of the phase prism. This also holds for short-chain nonionic amphiphiles for which the

(1) Kahlweit, M.; Strey, R.; Firman, P.; Haase, D.; Jen, J.; Schomäcker, R. *Langmuir* **1988**, *4*, 499.
(2) Kahlweit, M.; Strey, R. *Angew. Chem., Int. Ed. Engl.* **1985**, *24*, 654.
(3) Kahlweit, M.; Strey, R. *J. Phys. Chem.* **1987**, *91*, 1553.

0743-7463/89/2405-0305$01.50/0

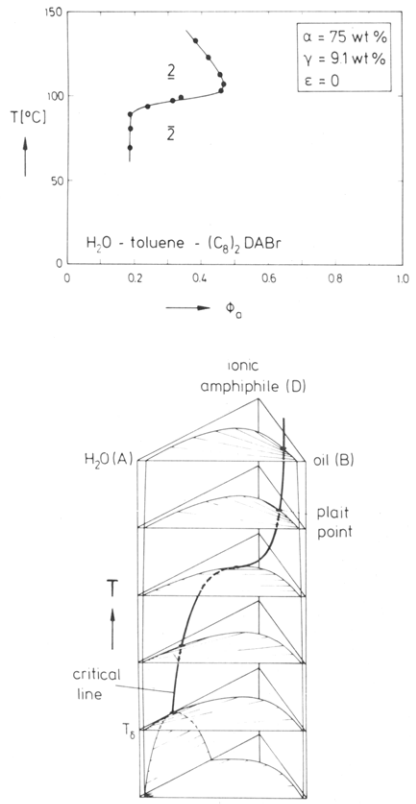

Figure 1. Top: volume fraction ϕ_a of the lower aqueous phase versus T for the mixture H_2O–toluene–$(C_8)_2DABr$, showing the change of distribution of the ionic amphiphile between water and oil with rising temperature. Bottom: phase behavior of a ternary mixture A–B–D represented in a phase prism with isothermal phase diagrams (schematic). The "connected" critical line changes from the water-rich to the oil-rich side with rising temperature.

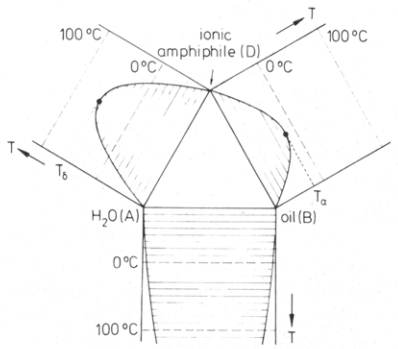

Figure 2. Unfolded phase prism of the ternary mixture A–B–D showing the phase diagrams of the corresponding binary mixtures (schematic).

tendency for phase separation is too weak to enforce the formation of an "upper loop".

Let us now consider the phase diagram of the A–D mixture. The upper critical temperature T_δ of their miscibility gap again depends on the nature of the amphiphile. It rises with increasing (effective) carbon number of the hydrophobic hydrocarbon chains and drops with increasing hydration energy of the hydrophilic ionic head group. Accordingly, one expects T_δ for single-tailed ionic amphiphiles to lie below the melting point but T_δ for double-tailed amphiphiles to lie above the melting point and even above the boiling point of the mixture. Experiments furthermore show that for comparable hydrophobic groups T_δ lies higher for cationic than for anionic amphiphiles. With rising temperature, water becomes an increasingly better solvent for ionic amphiphiles. As a consequence, A–D mixtures do not show an upper loop as A–C mixtures

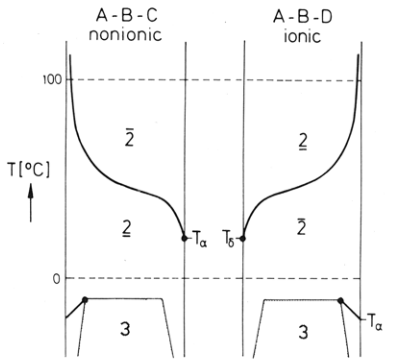

Figure 3. Trajectories of the connected critical lines projected from the amphiphile edge onto the A–B–T plane of the phase prism. Left: mixtures with nonionic amphiphiles. Right: mixtures with ionic amphiphiles (schematic).

do. At a temperature somewhat above T_δ, ionics, therefore, become more soluble in water than in oil, which makes the critical line change from the water-rich to the oil-rich side of the phase prism, as shown in the bottom of Figure 1.

For the further discussion we project the critical lines in the A–B–C and the A–B–D prism from the C and D edge, respectively, onto the A–B–T plane, as shown in Figure 3. Let us first discuss the critical lines in an A–B–C mixture with a short-chain nonionic amphiphile, that is, without an upper A–C loop (left). At temperatures below the melting point, the three lower miscibility gaps enforce the formation of a three-phase body. Since the critical temperature T_α of the B–C gap is assumed to lie above that of the lower A–C gap, this three-phase body will disappear at a temperature near the upper critical temperature of the lower A–C gap, with the critical end point lying on the water-rich side of the upper critical tie line. Between that temperature and T_α, isothermal phase diagrams show connected miscibility gaps extending from the A–B to the B–C side of the Gibbs triangle. At T_α, this gap disconnects from the B–C side; that is, a second critical line enters the phase prism on the oil-rich side. With further rising temperature water becomes an increasingly poorer solvent than oil for nonionic amphiphiles. As a consequence, the critical line changes from the oil-rich to the water-rich side of the phase prism. With short-chain nonionics that do not show an upper A–C loop, the critical line continues to ascend on the water-rich side until it terminates at the upper critical point of the A–B gap, well above the boiling point of the mixture.

Let us now consider the trajectories of the critical lines in an A–B–D mixture with an ionic amphiphile (right). Again the mixture will show a three-phase body at low temperatures. Since the upper critical temperature T_δ of the A–D gap is assumed to lie above that, T_α, of the B–D gap, the lower three-phase body will disappear at a temperature near T_α, the critical end point lying on the oil-rich side of the upper critical tie line. Between that temperature and T_δ, isothermal phase diagrams show connected miscibility gaps extending from the A–B to the A–D side. At T_δ, this gap disconnects from the A–D side; that is, a second critical line enters the phase prism on the water-rich side. With further rising temperature, water becomes an increasingly better solvent than oil for ionic amphiphiles. As a consequence, the critical line changes from the water-rich to the oil-rich side of the phase prism. With further rising temperature, the critical line continues to ascend on the oil-rich side until it terminates at the upper critical point of the A–B gap. The trajectory of the critical line of A–B–D mixtures thus resembles that of A–B–C mixtures without an upper loop, inversed, however, with

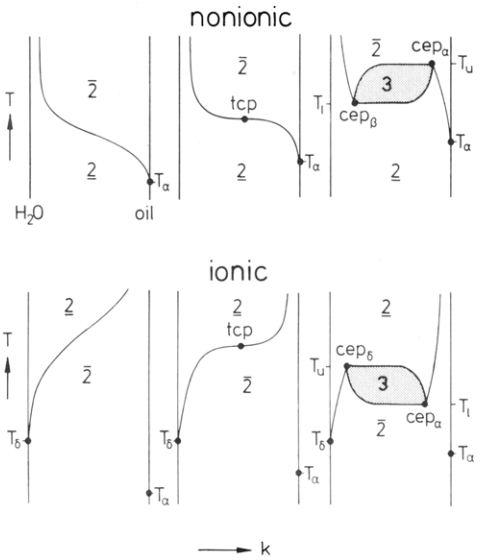

Figure 4. Formation of a three-phase body by breaking the connected critical line at a tricritical point (tcp) by increasing the carbon number k of the oil. Top: mixtures with nonionic amphiphiles. Bottom: mixtures with ionic amphiphiles (schematic).

respect to the water- and oil-rich sides.

In A–B–C mixtures, the lower critical temperature T_β of the upper A–C loop and the temperature of the inflection point of the critical line (often denoted by phase inversion temperature, PIT) are correlated. Correspondingly, one expects in A–B–D mixtures the upper critical temperature T_δ of the lower A–D gap and the temperature of the inflection point to be correlated. With single-tailed ionics, one, accordingly, expects the inflection point to lie below the melting point. With medium-chain double-tailed ionics it may lie either below or above the melting point, depending on the hydration energy of their head groups. With long-chain double-tailed ionics, one expects the inflection point to lie above the boiling point.

II. Formation of Three-Phase Bodies

We shall now consider the formation of a three-phase body within the phase prism. We disregard the three-phase bodies that arise from the interaction between the three lower miscibility gaps at this point and restrict the considerations to the formation of the three-phase bodies that arise from the inverse temperature dependence of the interaction between water and nonionic and ionic amphiphiles, respectively, close to the inflection points of the "connected" critical lines. As suggested by us in ref 2, a connected critical line can be looked at as an elastic spring, the bending tension of which can be increased by appropriately changing a field variable like the carbon number of the oil. Figure 4 shows on top the transition from a connected to a "broken" critical line for an A–B–C mixture and on bottom that for an A–B–D mixture, both schematic.

Increasing the carbon number k of the oil in A–B–C mixtures (Figure 4, top) leaves the A–C mixture unaffected but raises T_α, which decreases the tendency of the nonionic amphiphile to leave the water for oil. This raises the position of the inflection point, increasing the bending tension of the critical line. At a certain carbon number the critical line breaks at the tricritical point (tcp) which gives rise to the formation of a three-phase body. In A–B–D mixtures (Figure 4, bottom), increasing the carbon number of the oil leaves the A–D mixture unaffected but raises T_α, which increases the tendency of the ionic amphiphile to leave the oil for water. This lowers the position of the inflection point, increasing the bending tension of the critical line. At a certain carbon number, the critical line breaks at a tricritical point, which again leads to the formation of a three-phase body. For A–B–C mixtures, this was demonstrated experimentally in Figure 8 of ref 1. In such mixtures raising the temperature eventually enforces a separation of the lower aqueous phase at the critical end point, cep_β, into a water-rich phase (a) and an amphiphile-rich phase (c), which leads to the formation of isothermal three-phase triangles within the central miscibility gap. With a further rise in temperature, phase c moves on an ascending trajectory around the surface of the body of heterogeneous phases to the oil-rich side where it merges at cep_α with the oil-rich phase b, as shown in Figure 9 of ref 1. The three-phase body thus appears at T_l at the lower cep_β on the water-rich side and disappears at T_u at the upper cep_α on the oil-rich side. In the three-phase temperature interval

$$\Delta T \equiv T_u - T_l \tag{4}$$

the isothermal three-phase triangles change their shape such that phase c moves clockwise (if looked at from above) from cep_β to cep_α. With short-chain nonionic amphiphiles that do not show an upper A–C loop, the adjacent two-phase region on the water-rich side never touches the A–C side of the Gibbs triangle, whereas with nonionics that do show an upper loop, that two-phase region merges with that loop at $T = T_\beta$.

Ternary mixtures A–B–D with ionic amphiphiles show similar phase behavior as A–B–C mixtures without an upper loop. They are inversed, however, with respect to the water- and oil-rich sides. In such mixtures, raising the temperature eventually enforces a separation of the upper oil phase at cep_α into an oil-rich phase b and an amphiphile-rich phase c. This leads to the formation of isothermal three-phase triangles. With a further rise in temperature, phase c moves on an ascending trajectory around the surface of heterogeneous phases to the water-rich side, where it merges at cep_δ with the water-rich phase a. In A–B–D mixtures, the three-phase body thus appears at T_l at the lower cep_α on the oil-rich side and disappears at T_u at the upper cep_δ on the water-rich side. In the three-phase temperature interval ΔT, the isothermal three-phase triangles change their shape such that phase c moves counterclockwise (if looked at from above) from cep_α to cep_δ.

The phase behavior of A–B–D mixtures is thus equivalent to that of A–B–C mixtures but inverse with respect to the water- and oil-rich sides of the phase prism. In both mixtures, the three-phase bodies appear at a tricritical point and grow with increasing distance from the point. In A–B–C mixtures, however, their mean temperature rises with increasing carbon number of the oil, whereas in A–B–D mixtures, it drops.

III. "Simple" A–B–D Mixtures

The most convenient procedure for determining the positions and extensions of three-phase bodies is to erect a vertical section through the phase prism at constant α (e.g., α = 50 wt %) and then to observe the phase sequence with rising temperature. In ref 1 we demonstrated the essential features of the phase behavior of A–B–C mixtures by choosing the "simple" mixture H_2O–phenylalkanes (B_k)–C_4E_2 (see Figure 8 in ref 1). The binary mixture H_2O–C_4E_2 does not show an upper loop. With oils with a low effective carbon number k, the mixtures show connected critical lines. As one increases k, the critical line eventually breaks at a tricritical point, which leads to the formation of a three-phase body. With further increasing k, the three-phase temperature interval ΔT widens, and

its mean temperature $\bar{T}$, rises.

$$\bar{T} \equiv (T_l + T_u)/2 \quad (5)$$

We therefore, searched for an equivalently simple mixture with an ionic amphiphile for demonstrating the essential features of the phase behavior of A–B–D mixtures. As such we chose the mixture H_2O–aromatic oils–$(C_8)_2$DABr. This choice was triggered by studying the phase diagrams H_2O–$(C_m)_2$DAX (X standing for the counterion) published by Kunieda and Shinoda[4] with X = Cl^- and m = 12, 14, and 18 and by Evans and co-workers[5] with X = Br^- and m = 10 and 12. All phase diagrams show lamellar mesophases that are in equilibrium with isotropic micellar solutions. Both the lamellar region and the (lower) miscibility gap of the isotropic solutions drop temperaturewise with decreasing chain length m. Since experience shows that the lamellar region drops more rapidly than the A–D gap, we applied $(C_8)_2$DABr[6] because with this medium-chain amphiphile the lamellar mesophase has disappeared, leaving only the upper boundary of the lower A–D gap. This gap is shown in the right part of Figure 7. Its upper critical point cp_δ lies at T_δ = 20 °C and γ_δ = 32.3 wt %. The cmc was determined conductometrically and was found to be 2.5×10^{-2} M (γ = 0.88 wt %) at 25 °C, increasing slightly with rising temperature.

We then had to find an oil with a low (effective) carbon number with a sufficiently weak tendency to separate from the ionic amphiphile at elevated temperatures in order to find a connected critical line, as shown in the right part of Figure 3. As such we found benzene and toluene, which are both completely miscible with $(C_8)_2$DABr above the melting point of the binary mixture. With these oils one indeed finds (connected) critical lines that enter the phase prism at cp_δ, change to the oil-rich side with rising temperature to further ascend on that side (see Figure 1, top), and can be "broken" by increasing the carbon number, that is, by adding, e.g., xylene.

Although the phase behavior of quaternary mixtures should be represented in isothermal phase tetrahedra, we shall discuss that of the mixture H_2O (A)–oil (B_i)–oil (B_j)–ionic amphiphile (D) in a pseudoternary phase prism by combining the two oils into component B. For that purpose we introduce as a further composition variable the mass fraction of the oil with the higher effective carbon number ($k_j > k_i$) in the mixture of the two oils

$$\beta \equiv B_j/(B_i + B_j) \quad (6)$$

expressed in weight percent. Increasing β thus indicates increasing effective carbon number. The ternary mixture A–toluene–D is characterized by β = 0 wt % and the mixture A–xylene–D by β = 100 wt %.

On the left part of Figure 5 one can see vertical sections through the phase prism at α = 73.6 wt % with β as a parameter (in this particular quaternary mixture the three-phase bodies lie rather asymmetric to α = 50 wt % on the oil-rich side), to be compared with Figure 8 in ref 1. At elevated temperatures, the phase behavior was observed in sealed test tubes, that is, under slightly higher pressure. For β = 0 wt % (pure toluene) one finds a connected critical line that cuts a groove into the body of heterogeneous phases. As one increases β, that is, adds xylene, the groove becomes sharper until the critical line breaks close to β = 15 wt %. From then on one finds

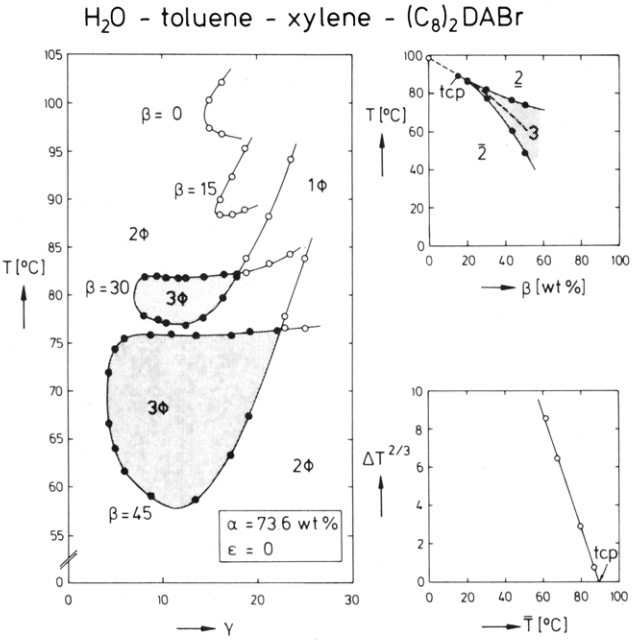

Figure 5. Evolution of a three-phase body. (Left) Vertical sections through the phase prism (α = 73.6 wt %) of the mixture H_2O–toluene–xylene–$(C_8)_2$DABr, β being the weight percent of xylene in the mixture of the two oils. Pure toluene (β = 0) shows a connected critical line with a two-phase body only. The critical line breaks at a tricritical point close to β = 15 wt %. With further increasing effective carbon number of the oil mixture of three-phase bodies drop and widen. Top right: three-phase temperature interval ΔT versus β, shaping a cusp that evolves from the tcp and descends with increasing β. Bottom right: $\Delta T^{2/3}$ versus mean temperature $\bar{T}$ of the three-phase body.

three-phase bodies that grow with increasing β, that is, with increasing effective carbon number k. With nonionic amphiphiles, $\bar{T}$ rises (see Figure 8 ref 1). With ionics, however, it drops, the three-phase bodies approaching the lower three-phase bodies that arise from the interaction between the three lower miscibility gaps.

In a quaternary mixture at constant pressure, a tricritical point is defined by its temperature, T_{tcp}, and its composition expressed in terms of a certain set of the variables α, β, and γ. For determining these coordinates one may proceed as in section III of ref 1; that is, start at a sufficiently high β and then measure ΔT and $\bar{T}$, gradually decreasing β and appropriately adjusting both α and γ. If plotted versus β, this should yield a cusp that ascends with decreasing β, terminating at the tcp. The upper right part of Figure 5 shows the cusp for this particular quaternary mixture, the tcp lying close to T = 89.5 °C, α = 73.8, β = 15.0, and γ = 11.6 wt %. Close to the tcp, all three phases show strong critical opalescence. Theory of near-tricritical mixtures[7] predicts that plotting $\Delta T^{2/3}$ versus $\bar{T}$ should yield a straight line with T_{tcp} as the foot point. This is indeed the case, as demonstrated in the lower right part of the Figure 5 (to be compared with Figure 10 of ref 8). If one applies benzene instead of toluene, one finds, as one would expect, a steeper cusp with a tcp at a higher β than with toluene but at about the same temperature.

If compared with the corresponding cusp for an A–B–C mixture (see right part of Figure 8 of ref 1), one finds that with nonionics the cusp evolves from a tcp at a low carbon number, ascending and widening with increasing k,

(4) Kunieda, H.; Shinoda, K. *J. Phys. Chem.* **1978**, *15*, 1978.
(5) Warr, G. G.; Sen, R.; Evans, D. F.; Trend, J. E. *J. Phys. Chem.* **1988**, *92*, 774.
(6) The amphiphile was synthesized in our laboratory by Dr. K.-H. Pospischil.
(7) See, e.g., Creek, J. L.; Knobler, Ch. M.; Scott, R. L. *J. Chem. Phys.* **1981**, *74*, 3489.
(8) Kahlweit, M.; Strey, R.; Firman, P.; Haase, D. *Langmuir* **1985**, *1*, 281.

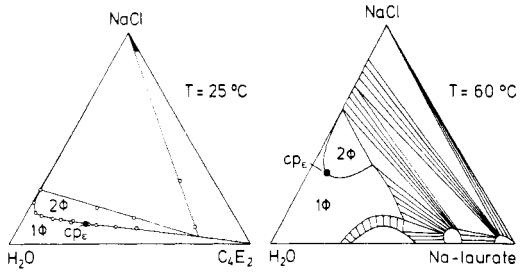

Figure 6. Left: isothermal phase diagram of the ternary mixture H_2O–C_4E_2–NaCl. Right: isothermal phase diagram of the ternary mixture H_2O–sodium laurate–NaCl (schematic after ref 9). NaCl "salts out" both nonionic and ionic amphiphiles.

whereas with ionics it descends with increasing β, that is, increasing effective carbon number. To our knowledge, the above three-phase bodies are the first found in a (pseudo)ternary A–B–D mixture without salt or cosurfactant.

IV. Effect of Inorganic Electrolytes

Instead of breaking the connected critical line by increasing the carbon number of the oil, that is, by appropriately changing its chemical potential, one may also break it by changing the chemical potential of the aqueous phase, that is, by adding an appropriate lyotropic salt (E). Quaternary mixtures H_2O–oil–amphiphile–salt are properly discussed in isothermal phase tetrahedra with the fourth component E on top. If the temperature is chosen such that the plait point of the phase diagram on the base of the tetrahedron lies on the oil-rich side, the formation of a three-phase body within that tetrahedron arises from the interaction between the central miscibility gap and a critical line that enters the tetrahedron at cp_ϵ in the triangle H_2O–amphiphile–salt. With A–B–C–E mixtures, one, therefore, has to chose temperatures below the inflection point of the connected critical line (of the ternary mixture) to find the plait point on the oil-rich side, whereas in A–B–D–E mixtures, one has to chose temperatures above the inflection point (see Figure 3).

We start by comparing the phase diagrams of the ternary mixtures A–C–E and A–D–E. The left part of Figure 6 shows the phase diagram of H_2O–C_4E_2–NaCl at 25 °C. C_4E_2 is completely miscible with water between its melting and boiling points. However, if one adds NaCl, the mixture separates in to two isotropic phases with a critical point, cp_ϵ, on the water-rich side. The effect of lyotropic salts on A–D mixtures has been extensively studied by McBain and co-workers. For example, we refer to a paper by McBain et al.[9] on the mixture H_2O–sodium laurate–NaCl. The right part of Figure 6 shows a schematic drawing of their Figure 4, showing the phase diagram at 60 °C. H_2O and sodium laurate form an isotropic solution at low amphiphile concentrations that separates into two isotropic phases upon addition of NaCl with a cp_ϵ on the water-rich side. In this respect, the A–C–E and the A–D–E diagrams show the same essential feature, namely, that adding a lyotropic salt makes both nonionic and ionic amphiphiles effectively more hydrophobic.

In mixtures with nonionic amphiphiles that do show an upper A–C loop, adding a salt makes the loop grow and, consequently, its lower critical temperature T_β drop. Or, in other words, the lower the temperature of application, the more salt has to be added to "salt out" the nonionic amphiphile. In mixtures with short-chain nonionic amphiphiles without an upper loop, adding a salt makes the loop appear and grow with further increasing salt concentration. This is demonstrated in the left part of Figure 7 for the ternary mixture H_2O–C_4E_2–NaCl. The pseudobinary phase diagrams were determined by dissolving the amphiphile in aqueous NaCl solutions of fixed concentration ϵ (in wt %). As one increases ϵ, T_ϵ drops whereas γ_ϵ decreases. By plotting T_ϵ (which plays the role of T_β in the ternary A–B–C mixture) versus ϵ, one finds the descending T_ϵ–ϵ trajectory shown in the upper left part of Figure 8.

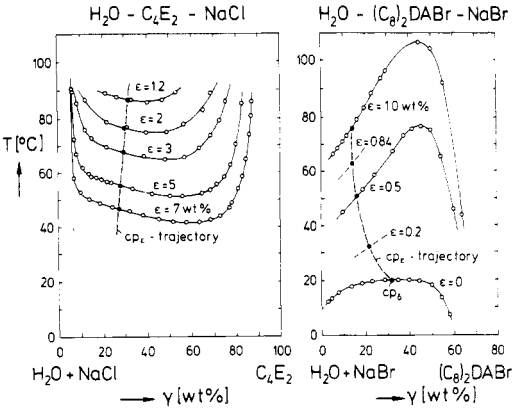

Figure 7. Left: pseudobinary phase diagram of the ternary mixture H_2O–C_4E_2–NaCl, showing the (lower) critical point cp_ϵ of the upper loop to drop with increasing salt concentration. Right: pseudobinary phase diagram of the ternary mixture H_2O–$(C_8)_2$DABr–NaBr, showing the (upper) critical point cp_ϵ of the lower gap to rise with increasing salt concentration.

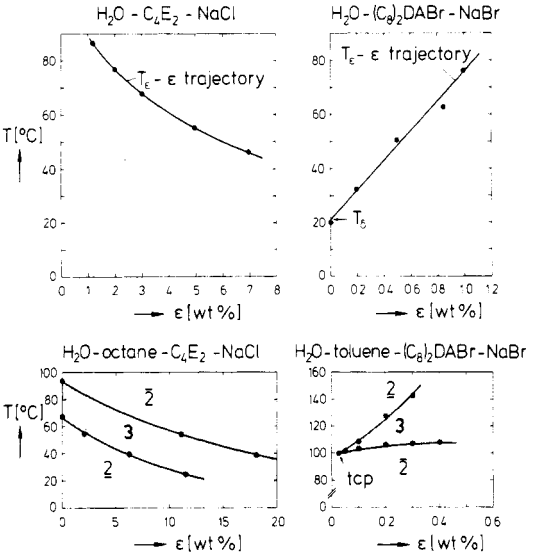

Figure 8. Top: T_ϵ–ϵ trejectories of the oil-free mixtures taken from Figure 7. Bottom left: salt cusp of the quaternary mixture H_2O–octane–C_4E_2–NaCl, apparently evolving from a tcp at a "negative" salt concentration and descending with increasing ϵ. Bottom right: salt cusp of the quaternary mixture H_2O–toluene–$(C_8)_2$DABr–NaBr, evolving from a tcp at $\epsilon > 0$ and ascending with increasing ϵ.

The same is true for mixtures with ionic amphiphiles, however, inverse with respect to temperature. Again adding salt makes the (lower) gap grow and, consequently, its upper critical temperature T_δ rise. Or, in other words, the higher the temperature of application, the more salt has to be added to salt out the ionic amphiphile. The right part of Figure 7 shows pseudobinary phase diagrams of the ternary mixture H_2O–$(C_8)_2$DABr–NaBr. The diagram for $\epsilon = 0$ is that for the binary mixture, cp_ϵ lying on top of the

(9) McBain, J. W.; Brock, G. C.; Vold, R. D.; Vold, M. J. *J. Am. Chem. Soc.* **1938**, *60*, 1870.
(10) Kahlweit, M.; Lessner, E.; Strey, R. *J. Phys. Chem.* **1984**, *88*, 1937.

miscibility gap. As one increases ϵ, T_ϵ rises and γ_ϵ decreases. By plotting T_ϵ (which plays the role of T_δ in the ternary A–B–D mixture) versus ϵ, one finds the ascending T_ϵ–ϵ trajectory shown in the upper right of Figure 8.

There is, however, an important difference between the effect of salt on the mutual solubility between H_2O and nonionic or ionic amphiphiles, respectively: with nonionics, the effect depends strongly on the nature of the anions;[11] that is, "structure builders" like SO_4^{2-} ions decrease the mutual solubility, whereas "structure breakers" like ClO_4^- increase it. With ionics, on the other hand, experience shows the effect to be essentially determined by the ionic strength, irrespective of the nature of the anions.

To enforce the formation of a three-phase body in A–B–C mixtures by adding salt, one has to choose a temperature below the inflection point of the critical line (see Figure 3). As one adds salt, the critical line cl_ϵ will eventually collide with the central gap within the phase tetrahedron. At that (lower) salt concentration ϵ, the lower aqueous phase separates into phases a and c. With a further increasing salt concentration, c moves to the oil-rich side were it merges with phase b at an (upper) salt concentration ϵ_u. The lower the temperature, the higher ϵ_l and the wider the three-phase salt interval

$$\Delta\epsilon \equiv \epsilon_u - \epsilon_l; \quad \delta T = 0 \tag{7}$$

Accordingly, $\Delta\epsilon$ shapes a cusp that descends temperaturewise as shown in the lower left part of Figure 8 for the mixture H_2O–*n*-octane–C_4E_2–NaCl. This mixture shows a three-phase body even at $\epsilon = 0$, suggesting the cusp to evolve from a tricritical point at a "negative" salt concentration. For salt cusps that evolve from a tcp at $\epsilon > 0$, see Figure 14 in ref 10.

To enforce the formation of a three-phase body in A–B–D mixtures by adding salt, one has to choose a temperature above the inflection point of the critical line. Again the amphiphile-rich phase (phase c) will appear at a certain ϵ_l and will disappear at a certain ϵ_u. In these mixtures, however, ϵ_l and $\Delta\epsilon$ increase with rising T. Accordingly, the three-phase salt intervals $\Delta\epsilon$ shape a cusp that ascends temperaturewise as shown in the lower right part of Figure 8 for the mixture H_2O–toluene–$(C_8)_2$DABr–NaBr. The salt cusp evolves from a tricritical point at $\epsilon > 0$, ascending and widening with increasing ϵ.

At constant temperature one thus finds in both mixtures the phase sequence $\underline{2} \rightarrow 3 \rightarrow \bar{2}$ with increasing salt concentration. The inverse shape of the cusps, however, leads to an inverse phase sequence if one varies temperature at constant brine concentration ϵ. In A–B–C–E mixtures one finds the sequence $\underline{2} \rightarrow 3 \rightarrow \bar{2}$ with rising temperature, whereas in A–B–D–E mixtures one finds the sequence $\bar{2} \rightarrow 3 \rightarrow \underline{2}$.

Alternatively, one may represent the phase behavior of a quaternary mixture in a pseudoternary phase prism by combining water and salt as "brine" is the A corner of the base. In such an (A + E)–B–C prism, cp_ϵ plays the role of cp_β, which is the lower critical point of the (A + E)–C loop. The critical line cl_β that enters the prism from the water-rich side terminates at the critical end point cep_β on the water-rich side of the lower critical tie line of the three-phase body, whereas the critical line cl_α ascends from temperatures below the three-phase body to terminate at cep_α on the oil-rich side of the upper critical tie line.

In an (A + E)–B–D prism, cp_ϵ plays the role of cp_δ, which is the upper critical point of the (A + E)–D gap. Accordingly, the critical line cl_δ terminates at cep_δ on the water-rich side of the upper critical tie line, whereas cl_α descends from temperatures above the three-phase body to terminate at cep_α on the oil-rich side of the lower critical tie line. This inverse phase behavior is demonstrated in the schematic diagrams of Figure 9.

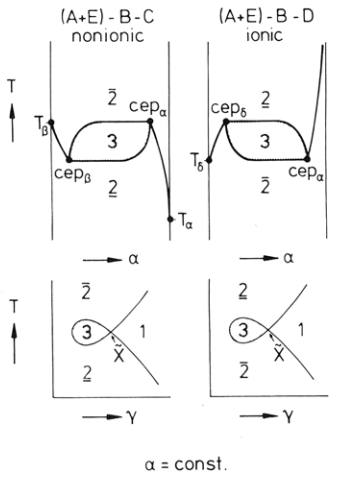

Figure 9. Vertical sections through pseudoternary phase prisms of A–B–C–E and A–B–D–E mixtures, respectively. Top: sections through the two critical end points (cep) of the three-phase bodies. Bottom: sections at constant water/oil ratio, that is, constant α (schematic).

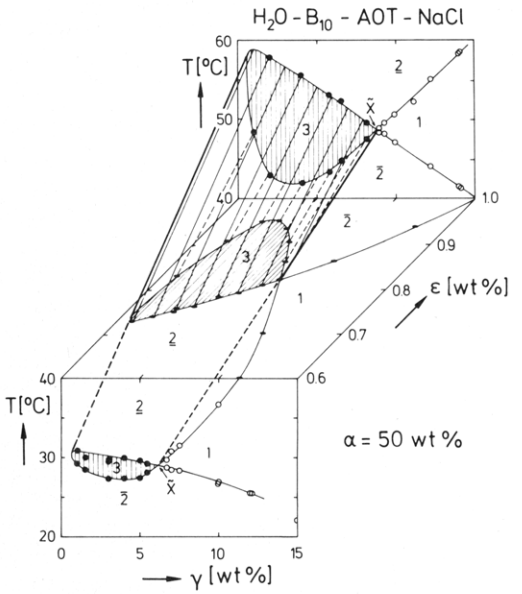

Figure 10. Three-phase body of the quaternary mixture H_2O–*n*-decane–AOT–NaCl in T–γ–ϵ space at α = 50 wt %, showing an isothermal section through that body at 40 °C.

Vertical sections through the two critical end points yield diagrams as shown in the top part of Figure 9. Such a section has been published by Kunieda and Shinoda[12] although not through the two cep's but at constant amphiphile concentration, that is, at constant γ. Vertical sections at constant α yield diagrams as shown in the bottom of Figure 9. In both mixtures the sections through the three-phase bodies resemble "fishes", however, with an inverse phase sequence. At point $\tilde{X}$, at which the three-phase body touches the homogeneous solution, one finds—for thermodynamic reasons[2]—the highest mutual solubility between water and oil. In mixtures with nonionic

(11) Firman, P.; Haase, D.; Jen, J.; Kahlweit, M.; Strey, R. *Langmuir* **1985**, *1*, 718.

(12) See, e.g., Figure 1 in Kunieda, H.; Shinoda, K. *J. Colloid Interface Sci.* **1980**, *75*, 601.

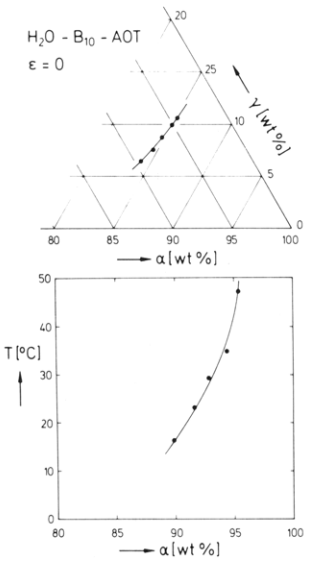

Figure 11. Trajectory of the critical line in the ternary mixture H_2O–*n*-decane–AOT ($\epsilon = 0$). Top: projected onto the A–B–D base. Bottom: projected from the D edge onto the A–B–T side of the phase prism.

amphiphiles, raising the temperature has the same effect as adding salt, that is, both drive the amphiphiles out of the aqueous into the oil-rich phase. With ionics, raising T has the opposite effect as adding salt. Rising T drives ionics out of oil into water, whereas salt drives them out of water back into the oil.

Figure 10 shows two vertical sections through the pseudoternary phase prism (H_2O + NaCl)–*n*-decane–AOT at α = 50 wt %, the one on the vertical plane in front determined at ϵ = 0.6 wt % and the one on the plane in the rear determined at ϵ = 1.0 wt %. In this T–γ–ϵ space, the three-phase body shapes a kind of a tube that ascends and widens with increasing ϵ, with the trajectory of point $\tilde{X}$ as a spur. A horizontal section through T–γ–ϵ space yields an isothermal section through the three-phase body at α = 50 wt %, again resembling the shape of a fish (see equivalent representation in T–γ–δ space for a mixture of a nonionic and an ionic amphiphile[13]). An alternative procedure for studying the effect of salt at constant temperature is to erect a section through the phase tetrahedron parallel to the A–B–E side at constant γ and then to determine the extensions of the three-phase body as they depend on α and ϵ. Such a section can be found in Figure 1 of ref 14 for the mixture H_2O–*n*-decane–AOT–NaCl at γ = 2 wt % and T = 42 °C, with the triangular section being represented in rectangular coordinates.

VI. Mixtures with Double-Tailed Anionic Amphiphiles

The last paragraph in the preceding section leads us to mixtures with double-tailed anionic amphiphiles. The most thoroughly studied double-tailed anionic amphiphile is AOT (sodium bis(2-ethylhexyl) sulfosuccinate) for which reason we first consider the phase behavior of quaternary mixtures H_2O–*n*-alkane (*k*)–AOT–NaCl. Their phase behavior can be readily understood by assuming both T_α and T_δ lie below the melting point, that is, by assuming the trajectories of the critical lines in the ternary mixture H_2O–*n*-alkane–AOT look essentially like those in the right part of Figure 3, except that both T_α and T_δ and thus the inflection points of the connected critical lines, lie close

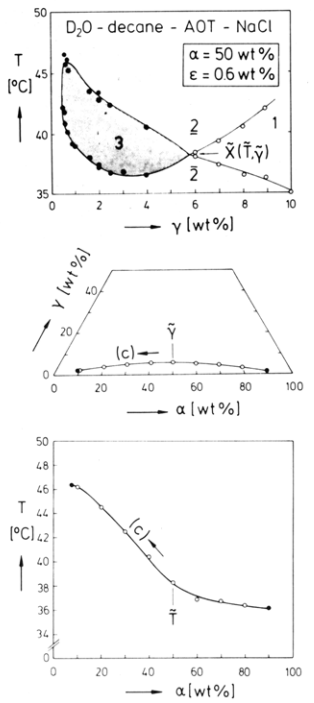

Figure 12. Trajectory of the amphiphile-rich phase c in the quaternary mixture D_2O–*n*-decane–AOT–NaCl. Top: vertical section through the pseudoternary phase prism at α = 50 wt % with point $\tilde{X}(\tilde{T},\tilde{\gamma})$ representing the locus of phase c at this particular value of α. Center: trajectory of phase c projected onto the base. Bottom: trajectory of phase c projected from the D edge onto the A–B–T side of the phase prism.

to or below the melting point, dropping temperaturewise with increasing carbon number. This is supported by Figure 11, which shows part of the trajectory of the (connected) critical line in the ternary mixture H_2O–*n*-decane–AOT ($\epsilon = 0$) in the oil-rich corner of the phase prism, on top projected onto the A–B–D base and on the bottom projected from the D edge of the prism onto its A–B–T side (to be compared with the inverse trajectory in an A–B–C mixture, Figure 3 of ref 1). Above the melting point, one thus finds the critical line (of the ternary mixture) to ascend on the oil-rich side with the solubility of water decreasing with rising temperature.

This explains why with AOT (and other anionic double-tailed amphiphiles of comparable effective carbon number) the only way to achieve three-phase bodies is to add a salt as a fourth component. This raises T_δ until the connected critical line breaks close to or even above the melting point of the quaternary mixture. Increasing the carbon number of the oils (at zero salt concentration) will not work because this will make the connected critical line break below its inflection point, that is, below the melting point.

Figure 12 shows on top a vertical section through the pseudoternary phase prism of the mixture (D_2O + NaCl)–*n*-decane–AOT at α = 50 wt % and ϵ = 0.6 wt % (to be compared with Figure 9 in ref 1), D_2O being applied for studying this particular mixture by SANS. Point $\tilde{X}$ represents the intersection of the trajectory of the amphiphile-rich phase c with the α = 50 wt % plane. At given α and ϵ, $\tilde{X}$ is unambiguously defined by the coordinates $\tilde{T}$ and $\tilde{\gamma}$. If ϵ is kept constant, one may determine $\tilde{X}$ at various α and thus follow the trajectory of phase c around the surface of the body of heterogeneous phases from the critical end point cep_α on the oil-rich side to cep_δ on the water-rich side. The center of Figure 12 shows the trajectory projected onto the base of the phase prism; the bottom of Figure 12 shows its projection from the D edge

(13) Kahlweit, M.; Strey, R. *J. Phys. Chem.* **1987**, *91*, 1553.
(14) Shinoda, K.; Kunieda, H. *J. Colloid Interface Sci.* **1987**, *118*, 586.

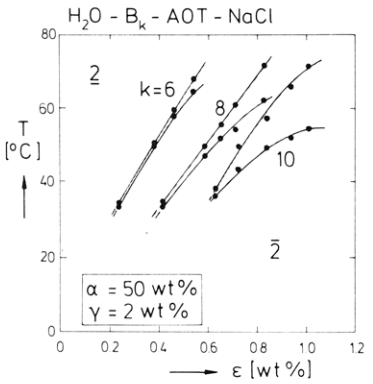

Figure 13. Salt cusps for H_2O–*n*-alkanes (k)–AOT–NaCl mixtures with carbon number k as a parameter (after ref 15).

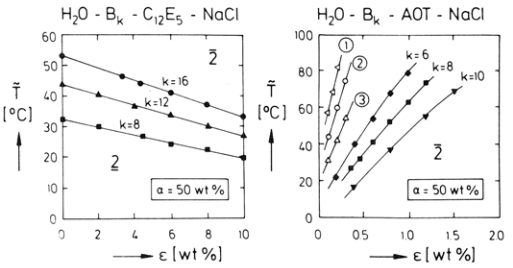

Figure 14. Left: $\tilde{T}$–ϵ trajectories for H_2O–*n*-alkanes (k)–$C_{12}E_5$–NaCl mixtures with carbon number k as a parameter. Right: $\tilde{T}$–ϵ trajectories for H_2O–*n*-alkanes (k)–AOT–NaCl mixtures with k as a parameter. Also shown are the trajectories for toluene (1), xylene (2), and mesitylene (3).

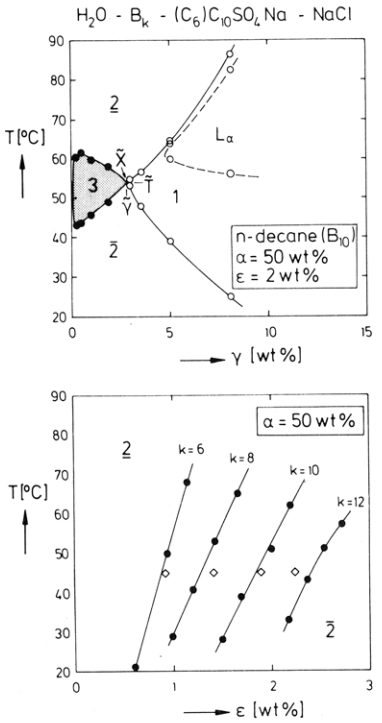

Figure 15. Phase behavior of H_2O–*n*-alkanes (k)–$(C_6)C_{10}SO_4Na$–NaCl mixtures. Top: vertical section through the pseudoternary phase prism with *n*-decane at α = 50 wt % and ϵ = 2 wt %. Bottom: $\tilde{T}$–ϵ trajectories at α = 50 wt % with carbon number k as a parameter. The open points were measured by Shinoda and Shibata.[18]

of the prism onto its (A + E)–B–T plane. In mixtures with nonionic amphiphiles (Figure 9 in ref 1), phase c moves from the water-rich to to oil-rich side with rising temperature, whereas in mixtures with ionic amphiphiles, it moves from the oil-rich to the water-rich side.

VII. Dependence on the Carbon Number of the Oils

In A–B–D mixtures, the inflection point of the critical line (see Figure 3) lies above the upper critical temperature T_δ of the A–D gap. With respect to the effect of the carbon number k of the oil on the position of the inflection point, one expects the temperature of the inflection point to drop with increasing k since the tendency of an ionic amphiphile to leave the oil-rich phase for the aqueous phase will be stronger the higher k. If a salt is added (at constant T), this drives the ionic amphiphile back into the oil-rich phase. Again one expects the "difficulty" for the electrolyte to drive the ionic amphiphile back into the oil to increase with increasing k. At constant temperature, one thus expects both ϵ_1 and $\Delta\epsilon$ to increase with increasing carbon number of the oil. This is confirmed by experiment. Figure 13 shows the salt cusps for some H_2O–*n*-alkane (B_k)–AOT–NaCl mixtures as determined by Kunieda and Shinoda at α = 50 wt % and γ = 2 wt %.[15]

Instead of measuring the extensions of the three-phase bodies at constant γ, one may characterize their position on the temperature scale by the $\tilde{T}$–ϵ trajectories at constant α. The right side of Figure 14 shows these trajectories for the cusps in Figure 13 as determined by us[16] to be compared with the corresponding trajectories for H_2O–B_k–$C_{12}E_5$–NaCl mixtures on the left. The trajectories for nonionic amphiphiles descend temperaturewise with increasing ϵ, whereas those for ionics ascend. In both cases the trajectories are shifted toward higher ϵ with increasing k. At constant brine concentration ϵ, one thus finds the three-phase bodies with nonionics to rise temperaturewise with increasing k, whereas those with ionics drop.

Extrapolating the trajectories on the right of Figure 14 to zero salt concentration, one finds the tricritical point of the mixture with decane to lie close to −10 °C, that with octane close to 0 °C, and that with hexane close to +10 °C. This finding suggests to apply aromatic oils since their effective carbon number is lower than that of *n*-alkanes. Accordingly, one expects the three-phase bodies with aromatic oils to lie at higher temperatures and lower salt concentration. This is indeed the case, as can be seen in the right part of Figure 14, which also shows the $\tilde{T}$–ϵ trejectories for mesitylene (3), xylene (2), and toluene (1).

This phase behavior is not a particular property of AOT but holds for all ionic amphiphiles of comparable effective carbon number that show a three-phase body in the "experimental window", that is, between the melting and boiling point of the mixtures. For example, the top of Figure 15 shows a vertical section through the pseudoternary phase prism of (H_2O + NaCl)–*n*-decane (B_{10})–$(C_6)C_{10}SO_4Na$, the latter standing for sodium 2-(*n*-hexyl)decyl sulfate[17] at α = 50 wt % and ϵ = 2 wt %. The dependence of the position of the three-phase body on the nature of the oil and the brine concentration is demonstrated in the bottom of Figure 15, which shows the $\tilde{T}$–ϵ trajectories for mixtures with $(C_6)C_{10}SO_4Na$ with the carbon number k of *n*-alkanes as a parameter. The empty points represent the position of the three-phase bodies as determined by Shinoda and Shibata.[18] As one can see, $(C_6)C_{10}SO_4Na$ shows essentially the same phase behavior as AOT, being, however, effectively more hydrophilic.

(15) Kunieda, H.; Shinoda, K. *J. Colloid Interface Sci.* **1980**, *75*, 601.
(16) Kahlweit, M.; Strey, R. *J. Phys. Chem.* **1988**, *92*, 1557.
(17) We are indebted to Dr. H. Sagitani from Pola Laboratories, Yokohama, for supplying us with the amphiphile.
(18) Shinoda, K.; Shibata, Y. *Colloid Surf.* **1986**, *19*, 185.

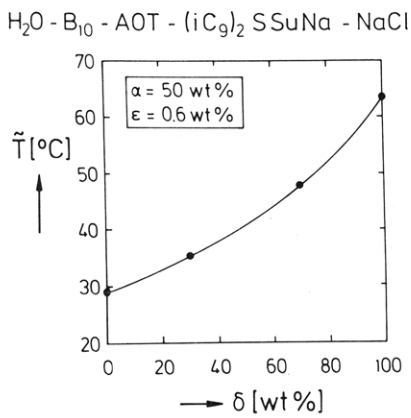

Figure 16. Mixtures of $(iC_8)_2SSuNa$ (AOT) with its longer chain homologue $(iC_9)_2SSuNa$. Shown is the $\tilde{T}$–δ trajectory for the quinary mixture H_2O–*n*-decane–AOT–$(iC_9)_2SSuNa$–NaCl at α = 50 wt % and ϵ = 0.6 wt %. δ Denotes the wt % of $(iC_9)_2SSuNa$ in the mixture of the two amphiphiles.

VIII. Dependence on the Chain Length of the Amphiphiles

The higher the effective carbon number k of the hydrophobic tail of the ionic amphiphile for a given ionic head group, the higher the critical temperature T_δ of the A–D gap. One thus expects the position of the inflection point of the (connected) critical line and, accordingly, that of the three-phase bodies to rise temperaturewise with increasing chain length of the amphiphile. For studying the effect of the chain length on the position of the three-phase body, we have applied mixtures of AOT (D) and the longer-chain homologue D′, (sodium bis(2-ethylheptyl) sulfosuccinate) abbreviated by $(iC_9)_2SSuNa$,[19] denoting the mass fraction of the longer chain amphiphile in the mixture of the two by

$$\delta \equiv D'/(D + D') \tag{8}$$

in weight percent. Increasing δ thus indicates increasing effective chain length of the mixture of the two amphiphiles. With *n*-decane (B_{10}) as oil and a brine concentration ϵ = 0.6 wt %, the three-phase body with AOT (D) lies at about 30 °C, with the longer chain D′ at about 60 °C. By mixing the two, one finds a smooth rise of $\tilde{T}$ with increasing δ at practically constant $\tilde{\gamma}$, as shown in Figure 16. In most applications, the temperature, the oil, and the brine concentration are given. The problem is to find that amphiphile the addition of which leads to the formation of a three-phase body under these particular conditions. One way to solve the problem is to mix two appropriately chosen amphiphiles as demonstrated in Figure 16 (for ionic amphiphiles) and Figure 14 of ref 1 (for nonionic amphiphiles).

Another example is shown in Figure 17. Here we have applied a mixture of D′ = $(C_7)C_9PhSO_3Na$ (Texas I) and the shorter chain homologue D = $(C_5)C_7PhSO_3Na$, again denoting the ratio between the two by δ. For the more hydrophilic D, the three-phase bodies with *n*-alkanes appear to lie below the melting point, whereas for Texas I (D′), they appear to lie above the boiling point. However, by mixing the two one may move the three-phase bodies into the experimental window. The top of Figure 16 shows a vertical section through the three-phase body for *n*-octane at α = 50 wt %, ϵ = 3.3 wt %, and δ = 45 wt %. On the bottom of Figure 17 one can see some $\tilde{T}$–ϵ trajectories of the mixture H_2O–*n*-octane–D–D′–NaCl with δ as a parameter. The trajectories move toward higher salt concentrations ϵ with decreasing δ, that is, dropping T_δ, which is in accord with the considerations presented in section IV.

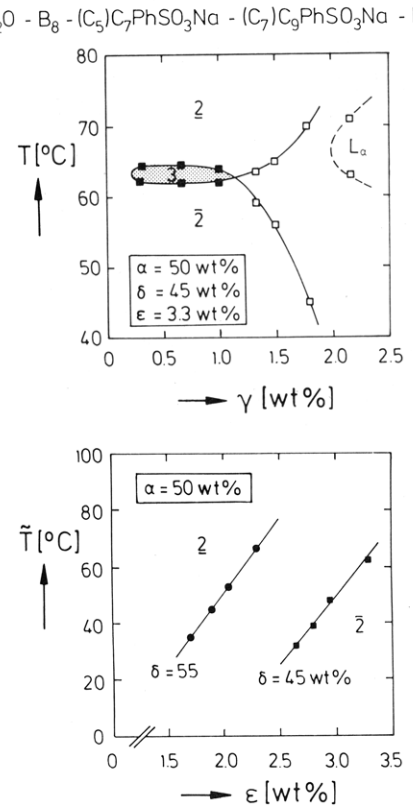

Figure 17. Mixtures of $(C_7)C_9PhSO_3Na$ (Texas I) with its shorter chain homologue $(C_5)C_7PhSO_3Na$, δ denoting the wt % of Texas I in the mixture of the two amphiphiles. Top: vertical section through the pseudoternary phase prism of the quinary mixture H_2O–*n*-octane–$(C_5)C_7PhSO_3Na$–Texas I–NaCl at α = 50 wt %, δ = 45 wt %, and ϵ = 3.3 wt %. Bottom: $\tilde{T}$–ϵ trajectories at α = 50 wt % for the above mixture with δ as a parameter.

If compared with the corresponding trajectories of mixtures with nonionic amphiphiles (see Figure 14 in ref 1), one again finds an inverse dependence on the hydrophilicity of the amphiphiles: with nonionics, the position of the three-phase bodies rises temperaturewise with increasing hydrophilicity of the amphiphile, whereas with ionics it drops.

This result suggests studying the effect of the branching of double-tailed ionic amphiphiles by changing the branching of the hydrophobic group from a double-tailed amphiphile of equal chain lengths stepwise to a single-tailed amphiphile, keeping the total number of carbon atoms constant. Experiments indicate that the three-phase bodies drop temperaturewise with decreasing symmetry of the two branches.[20] This would explain why with standard single-tailed anionic amphiphiles, in particular, it appears difficult to find a three-phase body in the experimental window even with the least hydrophobic aromatic oils by adding a lyotropic salt alone: T_δ and thus the inflection point of the ternary mixture A–B–D lie too far below the melting point. To enforce a separation into three phases within the experimental window one, therefore, has to change the (effective) chemical potential of the aqueous phase as well as that of the oil-rich phase by adding an appropriate fifth component that dissolves in both phases like a short-chain alcohol. Such weak nonionic

(19) The amphiphile was synthesized in our laboratory by R. Schmitz-Salue.

(20) Doe, P. H.; Wade, W. H.; Schechter, R. S. *J. Colloid Interface Sci.* **1977**, *59*, 525.

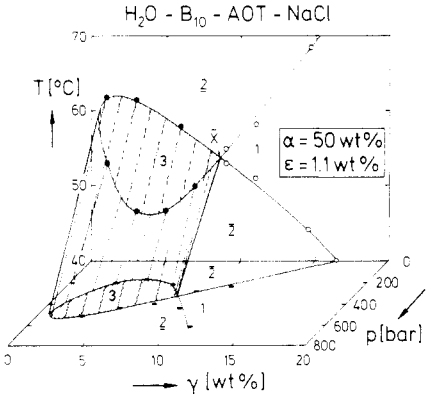

Figure 18. Effect of pressure on the phase behavior of the quaternary mixture H_2O–*n*-decane–AOT–NaCl, represented in T–γ–p space. The vertical plane in the rear shows a vertical section through the pseudoternary phase prism at α = 50 wt %, ϵ = 1.1 wt %, and 1 bar. The horizontal plane represents an isothermal section at 40 °C, showing the three-phase body to drop and shrink with increasing pressure.

amphiphiles may thus be considered either as co-surfactants or as co-oils. Their role in quinary mixtures depends on their amphiphilicity as well as on the temperature at which they are applied. We shall discuss this problem in more detail in a forthcoming paper.

IX. Effect of Pressure

As we have shown in ref 1, one may predict the effect of pressure on the position of the three-phase bodies by considering its effect on the two binary phase diagrams A–D and B–D. The position of the inflection point of the (connected) critical line in A–B–D mixtures is mainly determined by the position of the upper critical point cp_δ of the A–D gap and the phase separation tendency of the B–D mixture at elevated temperatures. For an upper critical point (T_δ), $\partial T_c/\partial p$ has the opposite sign of $\partial^2 V_m/\partial\gamma^2$, V_m denoting the mean molar volume of the mixture,[21] whereas for the critical line on the oil-rich side it has the same sign. Experience shows that the three-phase bodies drop temperaturewise with increasing pressure. This implies that $(\partial^2 V_m/\partial\gamma^2)_{\alpha=0} > 0$,[22] whereas little can be said about $(\partial^2 V_m/\partial\gamma^2)_{\alpha=100}$. One thus again finds an inverse behavior of nonionic and ionic amphiphiles: with nonionics, the three-phase bodies rise and widen with increasing pressure as shown in Figure 17 of ref 1. With ionics, however, they drop and shrink as shown in Figure 18 for the mixture H_2O–*n*-decane–AOT–NaCl (α = 50 wt %; ϵ = 1.1 wt %) in T–γ–p space. With nonionics, increasing pressure thus has the same effect as increasing salt concentration, whereas with ionics, increasing pressure has the same effect as decreasing ϵ, as can be seen by comparing Figure 18 with Figure 10.

X. Interfacial Tensions

With respect to the interfacial tensions betwen the three liquid phases of a three-phase body, one has to distinguish between two experimental procedures:

1. If the formation of the three-phase body is achieved by increasing the salt concentration ϵ at constant T, the lower phase separates into an aqueous (a) and an amphiphile-rich phase (c) at the (lower) salt concentration ϵ_l. With further increasing salt concentration, phase c moves from the water-rich to the oil-rich side, where it merges with the oil-rich phase b at the (upper) salt concentration ϵ_u. Consequently, the interfacial tension σ_{ac} starts from zero at ϵ_l to increase with further salt concentration, whereas σ_{bc} decreases with salt concentration to vanish at ϵ_u, as shown in the left part of Figure 19. In this experiment, mixtures with ionic amphiphiles show the same dependence of the interfacial tensions on ϵ as mixtures with nonionic amphiphiles.

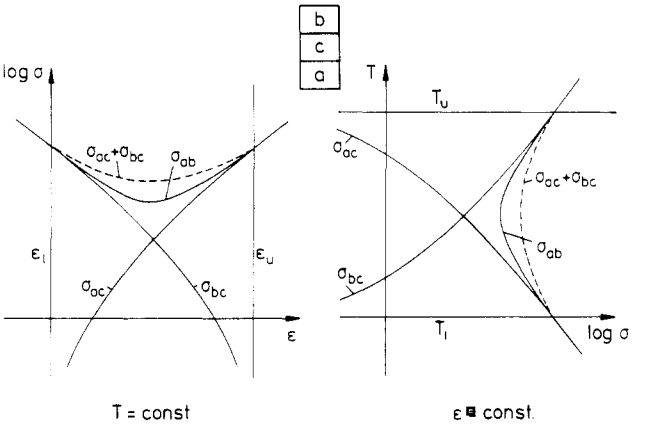

Figure 19. Interfacial tensions between the three liquid phases of a quaternary mixture A–B–D–E. Left: dependence of the interfacial tensions on brine concentration ϵ at constant T. Right: dependence of the interfacial tensions on T at constant ϵ. The broken lines represent the sum of σ_{ac} and σ_{bc} (schematic).

2. If the formation of a three-phase body is achieved by raising temperature at constant ϵ, the dependence of the interfacial tensions on T is inverse. With nonionics, phase c separates from a at T_l to merge with b at T_u (see Figure 19 in ref 1), whereas with ionics, phase c separates from b at T_l to merge with a at T_u. The corresponding interfacial tensions are shown in the right part of Figure 19.

In both cases the question arises whether or not the interfacial tension σ_{ab} between the aqueous and the oil-rich phase is equal or lower than the sum $\sigma_{ac} + \sigma_{bc}$. To answer that question, one does not have to measure the interfacial tensions, which can be time consuming. Instead one may carefully remove the amphiphile-rich phase c until only a tiny drop is left. This procedure does not change the chemical potentials of the three-phases but only their volume fractions within the three-phase triangle. If the drop of phase c spreads across the a/b interface, the equality holds. If, however, the drop shapes a lense floating on that interface, one has

$$\sigma_{ab} < \sigma_{ac} + \sigma_{bc} \tag{8}$$

Experiment shows that inequality 8 holds for all medium- and long-chain nonionic amphiphiles as well for all ionic amphiphiles hitherto studied, as demonstrated in Figure 4 of ref 23 for the mixture H_2O–*n*-decane–C_8E_3 and in Figure 20 for the mixture H_2O–*n*-decane–AOT–NaCl at 50 °C (initial composition before removing the middle phase: α = 50 wt %; γ = 4 wt %; ϵ = 1.0 wt %). We emphasize, however, that irrespective of whether the equality or the inequality (eq 8) holds, the interfacial tension σ_{ab} between the aqueous and the oil-rich phases must show a minimum near the mean temperature $\bar{T}$ (or the "optimum" salt concentration) of the three-phase body,

(21) Prigonie, I.; Defay, R. *Chemical Thermodynamics*; translated by Everett, D. H., Longmans: London, 1954; p 288ff.

(22) We recall that the cmc of ionic amphiphiles increases with increasing pressure, which implies that their partial molar volume is larger in the micellar state than in the monomeric state. See: Hamann, S. D. *J. Phys. Chem.* **1962**, *66*, 1359.

(23) Kahlweit, M.; Strey, R., Haase, D.; Firman, P. *Langmuir* **1988**, *4*, 785.

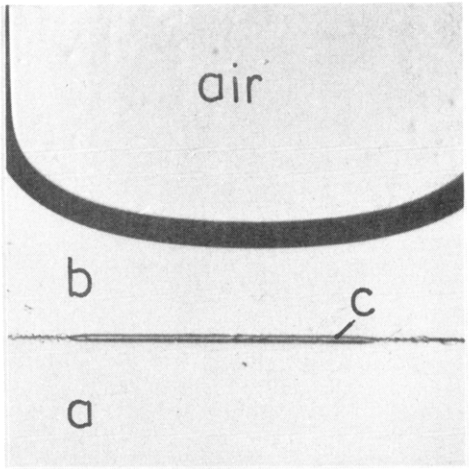

Figure 20. Drop of the amphiphile-rich phase c of the mixture H_2O–*n*-decane–AOT–NaCl at 50 °C, shaping a lens at the interface between the lower water-rich phase a and the upper oil-rich b, demonstrating the inequality $\sigma_{ab} < \sigma_{ac} + \sigma_{bc}$. The lens was produced in a thermostated optical cuvette of 1-mm thickness and observed through a horizontally mounted microscope. On top one can see the meniscus of the oil/air interface.

simply due to the nearness of two critical end points.

The characteristic dependence of the interfacial tensions on temperature (Figure 19) as well as the inequality (eq 8) have important consequences for the mutual wetting of the three liquid phases. This can be demonstrated by measuring the temperature dependence of the electric conductivity κ of a stirred (macro-) emulsion of the mixture (with a mean composition within the three-phase body). In a mixture with nonionic amphiphiles one has, for $T_l < T < \bar{T}$, $\sigma_{ac} < \sigma_{bc} < \sigma_{ab} < \sigma_{ac} + \sigma_{bc}$ but for $\bar{T} < T < T_u$, $\sigma_{bc} < \sigma_{ac} < \sigma_{ab} < \sigma_{ac} + \sigma_{bc}$. As a consequence, phase a tends to intrude between phases c and b below $\bar{T}$, whereas above $\bar{T}$, phase b tends to intrude between phases c and a. Below $\bar{T}$ a stirred emulsion, therefore, tends to build up a network of aqueous films between the droplets of c and b. Near $\bar{T}$, this network breaks down to be replaced by a network of oil-rich films between the droplets of phases c and a. If one adds a trace of an electrolyte to the mixture, one, therefore, finds below $\bar{T}$ a high conductivity of the stirred emulsion that breaks down rather abruptly near $\bar{T}$.

In a mixture with ionic amphiphiles, one has the inverse dependence of the relation between the interfacial tensions on temperature. Accordingly, one finds a low conductivity of a stirred emulsion below $\bar{T}$ that rises rather abruptly near $\bar{T}$. This inverse dependence of κ on T is demonstrated in Figure 21. In the upper left part of a Figure 21 a vertical section through the three-phase body of the mixture H_2O–*n*-tetradecane–$C_{12}E_4$[24] (with a trace of NaCl) at α = 50 wt % and in its upper right part κ versus T for the stirred emulsion. The lower part of Figure 21 shows a section through the three-phase body of the mixture H_2O–*n*-decane–$(C_6)C_{10}SO_4Na$–NaCl at α = 50 wt % and ϵ = 2 wt %, taken from Figure 15, and on its lower right part κ versus T. In both mixtures κ shows a rather abrupt jump close to $\bar{T}$. This effect has been frequently applied in practice for determining the so-called phase inversion temperature (PIT) of multicomponent liquid mixtures with either nonionic or ionic amphiphiles. Our experiments

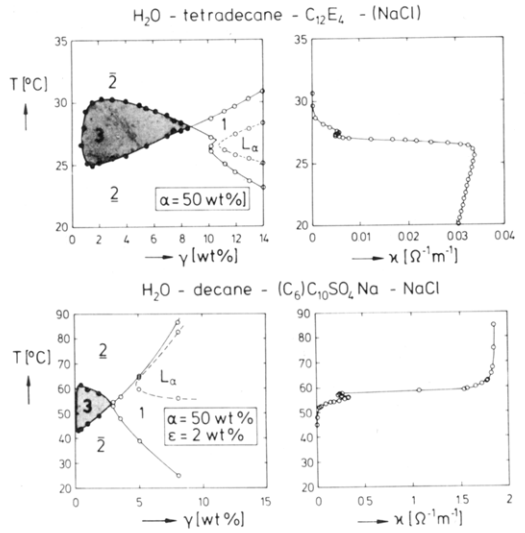

Figure 21. Electric conductivity in stirred macroemulsions with a mean composition within the three-phase body. Left: vertical sections through the phase prisms of the mixtures H_2O–*n*-tetradecane–$C_{12}E_4$ (with a trace of NaCl) and H_2O–*n*-decane–$(C_6)C_{10}SO_4Na$–NaCl, both at α = 50 wt %. Right: electric conductivity κ versus T, showing a jump of κ close to the mean temperature $\bar{T}$ of the corresponding three-phase bodies. The mixture with the nonionic $C_{12}E_4$ (measured at γ = 1.2 wt %) shows a sudden decrease of κ with rising temperature, whereas the mixture with the ionic amphiphile (measured at 0.5 wt %) shows a sudden increase. For further discussion see text.

demonstrate the reliability of this method. They, furthermore, show that the effect is apparently due to a (dynamic) wetting–nonwetting transition as a consequence of the peculiar temperature dependence of the relations between the interfacial tensions. With respect to the effect of these relations on the viscosity of such macroemulsions and the velocity of their separation into three liquid layers we refer to ref 25.

XI. Conclusion

After having presented qualitative thermodynamic descriptions of the general patterns of the phase behavior of liquid mixtures with nonionic[1] and ionic (this paper) amphiphiles, respectively, as well as that with mixtures of nonionic and ionic amphiphiles,[16] we shall in a forthcoming paper consider the role of so-called "cosurfactants". On the basis of these studies we shall then suggest how to chose appropriate mixtures of amphiphiles for achieving three-phase bodies with low $\tilde{\gamma}$, that is, high efficiency of the amphiphiles, if the temperature, the oil, and the brine concentration are given.

Acknowledgment. We are indebted to B. Faulhaber, T. Lieu, J. Winkler, and A. Ellrott for their assistance with the experiments, to D. Luckmann for drawing the figures, and to the German Federal Ministry for Research and Technology (BMFT) for financial support (Grant No. 0326315 B).

Registry No. $(C_8)_2$DABr, 3026-69-5; AOT, 577-11-7; $(C_7)C_9PhSO_3Na$, 67267-95-2; $(C_5)C_7PhSO_3Na$, 2212-52-4; NaCl, 7647-14-5; toluene, 108-88-3; benzene, 71-43-2; xylene, 1330-20-7; decane, 124-18-5.

(24) Kunieda, H., unpublished measurement.

(25) Kahlweit, M. et al. *J. Colloid Interface Sci. 1987*, 118, 436